ELSEVIER

Journal of Power Sources 72 (1998) 165–173

JOURNAL OF POWER SOURCES

Electrochemical impedance spectra of full cells: Relation to capacity and capacity-rate of rechargeable Li cells using $LiCoO_2$, $LiMn_2O_4$, and $LiNiO_2$ cathodes

Jiang Fan [1], Peter S. Fedkiw [*]

Department of Chemical Engineering, North Carolina State University, Raleigh, NC 27695-7905, USA

Received 7 July 1997; accepted 5 September 1997

Abstract

Electrochemical impedance spectra (EIS) are reported for rechargeable lithium cells using cathodes LiM_yO_x (M = Co, Ni, and Mn) prepared from casting and high-pressure compacting. The composite cathodes were cast from a slurry mixture consisting of 30% NMP solvent and 70% solid (91% LiM_yO_x, 3% PVDF and 6% KS44 graphite) onto a 25-μm thick Al current collector. The compacted cathodes were made from the cast cathode using a laboratory press. The most compacted cathodes have the smallest impedance and the highest specific capacity and capacity-rate. Three equivalent circuits are proposed according to the effect of compaction pressure on our EIS results and work reported in the literature. The EIS results and relationship to the capacity and capacity-rate are discussed using these circuits. It appears that the ohmic resistance of the composite cathode is an important factor in the overall resistance of the cell and unfavorably affects the performance (capacity and capacity-rate) of the cathode. © 1998 Elsevier Science S.A.

Keywords: Impedance spectroscopy; Lithium battery; Metal-oxide cathode

1. Introduction

Electrochemical impedance spectroscopy (EIS) is useful in studying rechargeable lithium cells [1–8], and EIS studies have led to a better understanding of many aspects of a lithium cell such as failure mechanism [1,2], self discharge [3], lithium-cycling efficiency [4,5], interfacial phenomenon between electrode and electrolyte [6,7], and lithium cation diffusion in electrode and electrolyte [8]. However, since there are no generally accepted equivalent circuits for lithium batteries, it is clear that we are still far from understanding completely their EIS response. Such a situation is probably due to EIS studies being affected by many factors. For example, it has been found [1–8] that EIS can be affected by electrolyte, lithium, cathode materials, discharge state, and even the cycle number. Among these, the cathode perhaps has been given the least attention, partially because problems related to the lithium anode are the main concern for commercialization of rechargeable lithium batteries. But, with progress in lithium and lithium-ion battery technology, attention is shifting gradually to the cathode and related problems.

It is recognized [9–11] that the capacity of rechargeable lithium batteries (including lithium-ion) is limited by the capacity of the cathode. For instance, for lithium-ion batteries, the capacity of a graphite anode can be as high as 570 mAh/g with small irreversible capacities [9]. This value is much higher than capacities obtained from conventional cathodes such as $LiCoO_2$, $LiMn_2O_4$, and $LiNiO_2$, which are 137, 148 and 192 mAh/g, respectively [12]. Clearly, increased capacity for lithium batteries, to a large degree, depends on the development of a high-capacity cathode. In fact, searching for a high-capacity cathode is an active research area [9–11]. Some new materials have emerged, for example, V_2O_5 aerogel [11] is reported to have a specific capacity as high as 550 mAh/g and a specific energy of ~1750 Wh/kg (for comparison, ~600 Wh/kg for both $LiCoO_2$ and $LiNiO_2$); unfortunately, however, its cycle life must be improved before it can become commercial.

It is important to understand the factors governing the capacities of conventional composite cathodes based on

[*] Corresponding author. E-mail: fedkiw@eos.ncsu.edu
[1] Present address: Polystor Corp., Dublin, CA 94568, USA.

0378-7753/98/$19.00 © 1998 Elsevier Science S.A. All rights reserved.

$LiCoO_2$, $LiMn_2O_4$ or $LiNiO_2$ in order to take full advantage of these materials. The battery industry has done tremendous work in optimizing the performance of these conventional cathodes, but it is generally kept as a trade secret. Nevertheless, there is some information published in the literature. For instance, Kanno et al. [13] found that there is an optimum amount of graphite which will yield the highest capacity for a composite cathode based on $LiNiO_2$; Huang [14] found that the capacity increases with a decrease in $LiMn_2O_4$ particle size.

The objectives of the present study are: (i) to understand contributions from the composite cathodes to EIS of rechargeable lithium cells by comparing EIS results obtained using different cathode materials with different preparation methods, and (ii) to understand the relationship between EIS of a cell and its capacity or capacity-rate. We hope that these EIS studies combined with full-cell testing may (i) lead to a better understanding about the effects of components and preparation of a composite cathode on cell performance, (ii) enable a way to gauge cathode performance before full-cell testing, and (iii) help to prepare high-performance cathodes for rechargeable lithium and lithium-ion batteries.

2. Experimental

Ethylene carbonate (EC) and dimethyl carbonate (DMC) were obtained from Aldrich. The mixed solvent EC:DMC (50%:50% [vol.]) was dried in 4 Å molecular sieve for ~2 weeks before use. $LiPF_6$ was used as received. A 1 M $LiPF_6$ EC:DMC solution was made in an Ar-filled glove box. The water content in the solution was 13 ppm, as determined by coulometric Karl Fisher titration. The Celgard 2500 separator was obtained from Hoechst Celanese.

$LiCoO_2$ was obtained from Alfa. $LiNiO_2$ was obtained from Honjo Chemical (Japan). $LiMn_2O_4$ was obtained from Merck (Germany). Poly (vinylidene fluoride) (PVDF (KYNAR)) was obtained from Elf Atochem. KS 44 Graphite was obtained from Timcal American. The 1-methyl-2-pyrrolidinone (NMP) was obtained from Fisher Scientific.

Typically, about 15 g of the mixture 91% (wt.) metal oxide, 6% KS44 graphite and 3% PVDF were mixed with about 8 g of 1-methyl-2-pyrrolidinone in a 30 ml polypropylene bottle, then the sealed bottle was put into a mixer for about 12 h. The resulting slurry was cast onto a 0.025-mm thick Al foil placed on a sheet of glass, and a doctor blade set sequentially to a gap of 0.25 mm and 0.20 mm was used to define the thickness. The resulting film was dried in a vacuum oven at ~120°C for ~24 h, then was cut into a ~0.75-cm diameter disk which was hot-compacted by a hydraulic press at ~150°C. After compaction, the cathode was dried again in a vacuum oven at ~150°C for ~24 h. The thicknesses of the cast cathode and cathodes compacted under 270 and 540 bar were measured using a Mitutoyo micrometer and are summarized in Table 1.

Table 1
Thickness of the cathodes

Pressure (bar)	$LiCoO_2$ (mm)	$LiMn_2O_4$ (mm)	$LiNiO_2$ (mm)
0 (cast cathode)	0.085–0.092	0.076–0.092	0.076–0.097
270	0.064–0.073	0.065–0.072	0.058–0.071
540	0.061–0.063	0.061–0.065	0.056–0.065

The range of measured thickness on a sample is reported.

A button cell was assembled in an Argon filled glove box. The following procedure was employed: (i) a Teflon ring gasket was placed into the bottom can; (ii) a ~1.5-cm diameter composite cathode disk was put into the bottom can (the cathode disk contains ~0.016 g (~2.4 mAh) $LiCoO_2$, or ~0.018 g (~2.6 mAh) $LiMn_2O_4$, or ~0.021 g (~4 mAh) $LiNiO_2$); (iii) a ~1.7-cm diameter separator (Celgard 2500) was placed concentric on the face of the cathode; (iv) the liquid electrolyte (~0.06 ml) was loaded on the surface of the separator; (v) a ~1.5-cm diameter lithium disk (~0.75-mm thick, weighing ~0.075 g, ~285 mAh) was put on top of the separator; (vi) a home-made spring (using Chromel A, B & S size 26, Hoskins, Detroit) was placed on top of the lithium disk; (vii) a lid can was placed on the top of the spring; and finally; (viii) the button cell was compressed and sealed using a home-made, button-cell press. The impedance was measured on a discharged cell using the PAR M398 impedance software to control a PAR Model 273 potentiostat and an EG&G Model 5210 lock-in amplifier in the frequency range 0.1 Hz to 100 kHz. The EIS data were fit by the Equivalent Circuit software (Version 3.96) supplied by EG&G. The full-cell cycling tests at constant charge or discharge current were carried out using an Arbin battery cycler (Model BT2042).

3. Results

Fig. 1 shows EIS results of lithium cells at their discharged state using a $LiNiO_2$ cathode (a) cast, (b) 270-bar compacted, and (c) 540-bar compacted. The inset in Fig. 1b is an enlargement of the region below 60 Ω and that on Fig. 1c is an enlargement below 80 Ω. The cell using the cast cathode shows large impedances at low frequencies. The line (in this and all Nyquist diagrams) is the best-fit result using the proposed equivalent circuit, which is discussed later. The EIS of the cycled cells was obtained after three cycles at $C/40$ (~0.057 mA/cm^2) followed by four cycles at $3C/40$ rate (~0.17 mA/cm^2). The resistance (i.e., the radius of Arc A and Arc B) decreases with increase in compaction pressure for the uncycled cells, but it appears independent of pressure for the cycled cells.

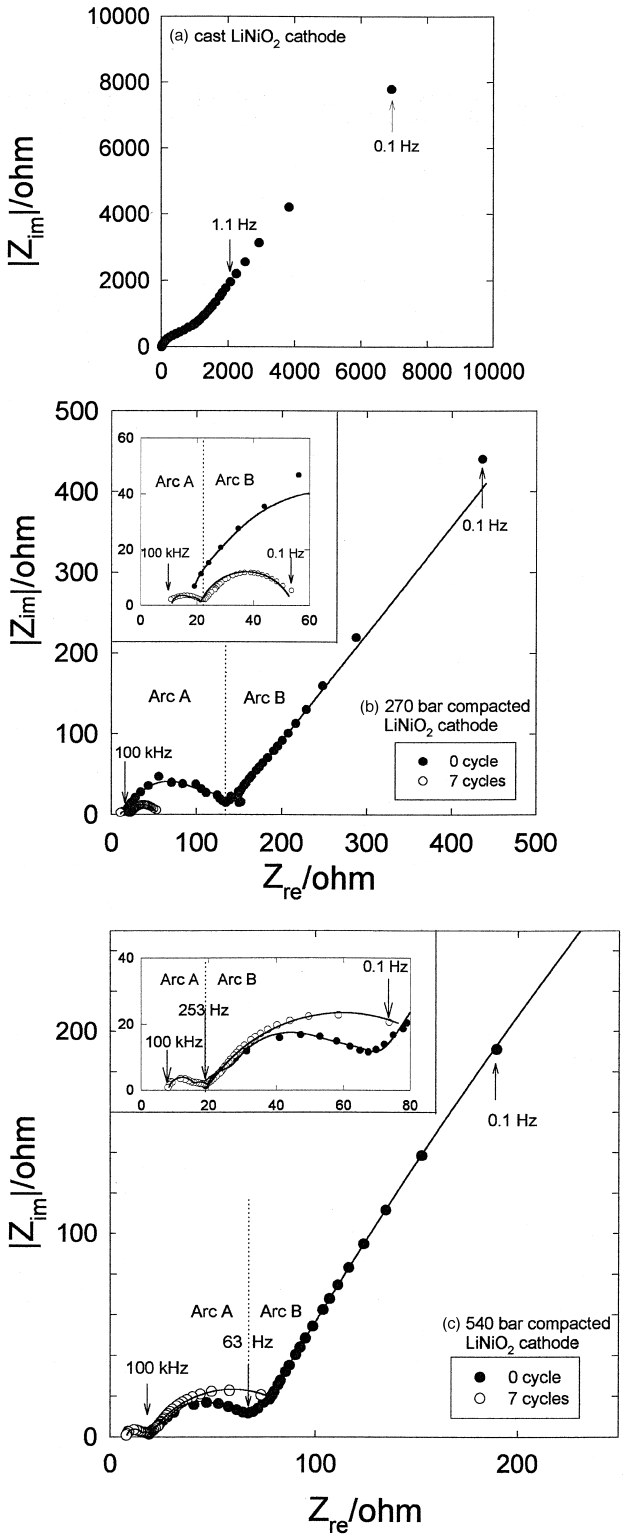

Fig. 1. EIS of discharged lithium cells after 0 and 7 charge–discharge cycles. The cells use a $LiNiO_2$ cathode prepared from (a) casting, (b) 270-bar compaction, and (c) 540-bar compaction. The vertical dashed line intersecting the cusp-like point on the solid line demarcates the boundary of Arcs A and B. Thus, in the inset of (b) and (c), the two arcs are shown for the cycled cell and the main figure indicates the same for the uncycled cell.

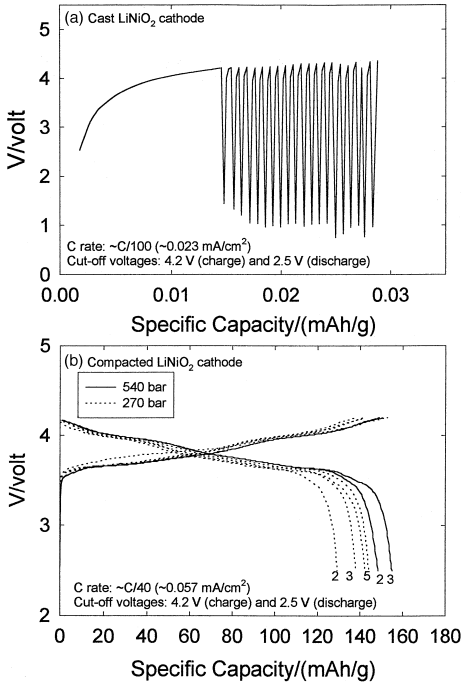

Fig. 2. Charge and discharge behavior of rechargeable lithium cells using a $LiNiO_2$ cathode prepared from (a) casting, and (b) 270- or 540-bar compaction. The voltage drops below the set-point of 2.5 V on discharge because data acquisition and control speed is not sufficiently fast.

Most of the EIS results obtained in this study may be divided into two arcs: Arc A corresponds to the higher-frequency semicircle (typically, 300 Hz $< \omega$), and Arc B corresponds to the lower-frequency semicircle (typically, 0.1 Hz $< \omega <$ 10 Hz). Note that Arc B for the uncycled cells does not develop fully in the measured frequency range.

The uncompacted-cathode cell could not be cycled, e.g., Fig. 2a shows the unstable behavior using a cast $LiCoO_2$ cathode at $C/100$; Fig. 2b shows, in contrast, the well-behaved, charge-discharge behavior for a cathode compacted at 270 or 540 bar. The cell using a 540-bar-compacted cathode showed the largest capacity, which can be seen more clearly in the capacity dependence on cycle number shown in Fig. 3. After $\sim$7 cycles, the cell using a 540-bar-compacted cathode has a $\sim$15% higher capacity than the cell using a 270-bar-compacted cathode.

Fig. 4 shows the specific-capacity dependence on the capacity-rate (C rate) for uncycled and cycled lithium cells using 540-bar-compacted $LiNiO_2$, $LiCoO_2$ or $LiMn_2O_4$ cathodes. An uncycled cell in this context means that the cell was discharged for the first, second, or third time (see caption). The capacity decreases more rapidly with increasing C rate for the $LiNiO_2$ fresh cell than for its corresponding cycled cell. This phenomenon can be correlated to the large difference in the radius of Arc B in the Nyquist diagram for the cycled and uncycled cells seen in Fig. 1. This correlation suggests that Arc B is somehow related to lithium diffusion within the composite cathode

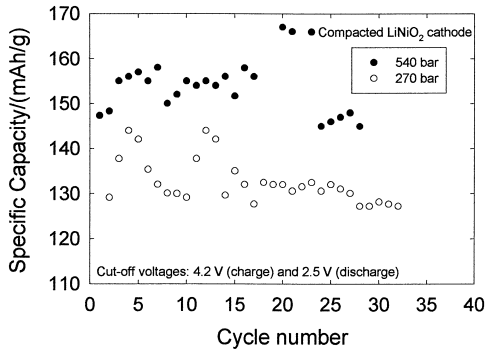

Fig. 3. Capacity dependence on cycle number for lithium cells using a $LiNiO_2$ cathode at various C rates. For the $LiNiO_2$, cathode compacted at 270 bar, ~145 and ~130 mAh/g capacities were obtained with $\sim C/40$ (~ 0.057 mA/cm^2) and $\sim 3C/40$ (~ 0.17 mA/cm^2) rates, respectively. For the $LiNiO_2$ cathode compacted at 540 bar, ~167, ~155, and ~149 mAh/g capacities were obtained with $\sim C/40$ (~ 0.057 mA/cm^2), $\sim C/20$ (~ 0.11 mA/cm^2), and $\sim 3C/40$ (~ 0.17 mA/cm^2) rates, respectively.

because lithium diffusion determines the C rate [15]. In contrast, the capacity dependence on C rate was similar for the uncycled and cycled cells using $LiCoO_2$ and $LiMn_2O_4$ cathodes. Correspondingly, there is a much smaller difference in the radii of Arc B for these two materials. We will discuss this phenomenon later in detail.

Fig. 5 shows the EIS results of lithium cells at their discharged state using $LiCoO_2$ cathodes prepared from (a) casting; (b) 270-bar compaction; and (c) 540-bar compaction. The EIS of the cycled cells were obtained after 15 cycles at a $C/12$ rate (~ 0.11 mA/cm^2). Similar to the cell using a $LiNiO_2$ cathode, the resistance is very large for the cell using the cast cathode. The resistance (radius of Arc A and B) decreases with increase in compaction pressure for the uncycled cells, but it becomes similar for the cycled cells. Arc A for the cycled cells seems to be better-defined than those of the uncycled cells.

Fig. 6 shows the charge and discharge behavior of lithium cells using a $LiCoO_2$ cathode prepared with 270-

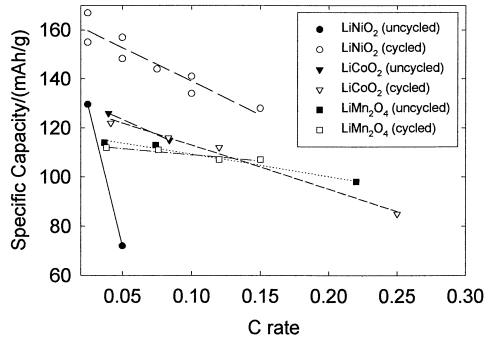

Fig. 4. Specific capacity dependence on capacity-rate for rechargeable lithium cells using $LiNiO_2$, $LiCoO_2$, and $LiMn_2O_4$ cathodes compacted at 570 bar. The results for 'uncycled' cells are for the initial discharge at the specified C rate and were obtained at sequentially decreasing rate. The results for cycled cell were obtained after at least seven cycles.

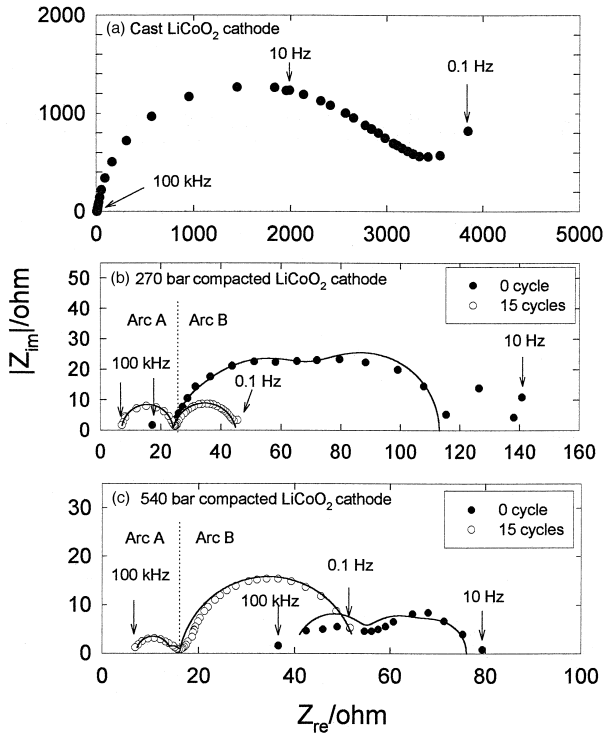

Fig. 5. EIS of discharged lithium cells after 0 and 15 charge–discharge cycles. The cells use a $LiCoO_2$ cathode prepared from (a) casting, (b) 270-bar compaction, and (c) 540-bar compaction.

or 540-bar compaction. It was found (not shown) that a cell using a cast cathode could not be charged and discharged, even at a rate as slow as $C/100$ (~ 0.014 mA/cm^2). The cell using a 540-bar-compacted cathode shows a relatively high capacity, which is seen more clearly in Fig. 7. After ~12 cycles, the cell has a ~12% higher capacity than that using a 270-bar-compacted cathode.

Fig. 8 shows the EIS results of lithium cells at their discharged state using a $LiMn_2O_4$ cathode prepared from (a) casting; (b) 270-bar compaction; and (c) 540-bar compaction. The EIS of the cycled cells was obtained after eight cycles at a $C/13$ rate (~ 0.11 mA/cm^2). Similar to

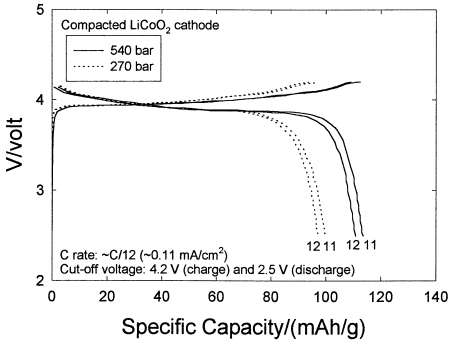

Fig. 6. Charge and discharge behavior of rechargeable lithium cells using a $LiCoO_2$ cathode prepared with 270- or 540-bar compaction.

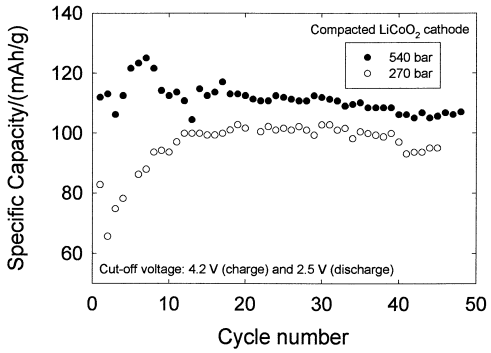

Fig. 7. Capacity dependence on cycle number for lithium cells using a $LiCoO_2$ cathode. For the $LiCoO_2$ cathode compacted at 270 bar, the capacity-rate was $C/24$ (~ 0.057 mA/cm^2) from the 1st to 4th cycle and $\sim C/12$ (~ 0.11 mA/cm^2) afterwards. For the $LiCoO_2$ cathode compacted at 540 bar, the capacity-rate was $C/24$ (~ 0.057 mA/cm^{-2}) from the 5th to 8th cycle and $\sim C/12$ (0.11 mA/cm^2) afterwards.

the other two cathode materials, the impedance for the cell using the cast cathode is large at low frequencies. Again, the resistance (radius of Arc A and Arc B) decreases with increase in compaction pressure for the uncycled cells, but becomes similar for the cycled cells.

Fig. 9 shows the charge and discharge behavior of lithium cells using a cast $LiMn_2O_4$ cathode compacted at

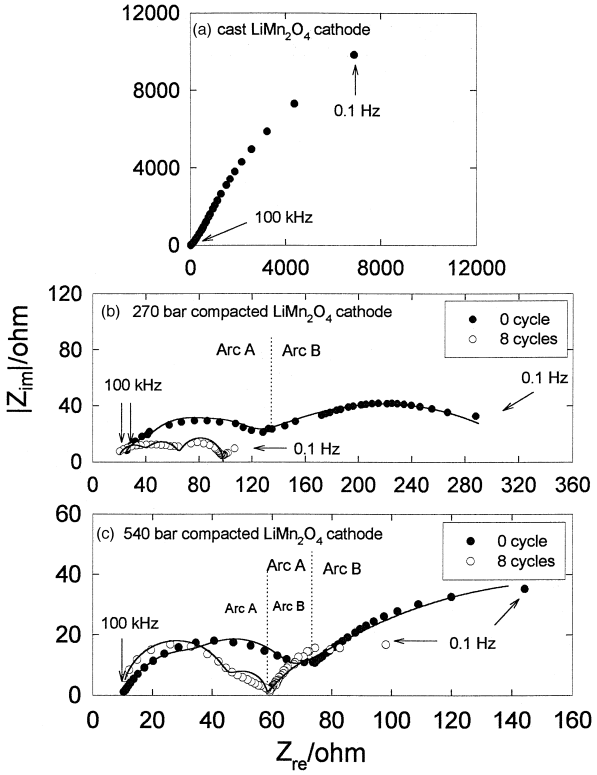

Fig. 8. EIS of discharged lithium cells after 0 and 8 charge–discharge cycles. The cells use a $LiMn_2O_4$ cathode prepared from (a) casting, (b) 270-bar compaction, and (c) 540-bar compaction.

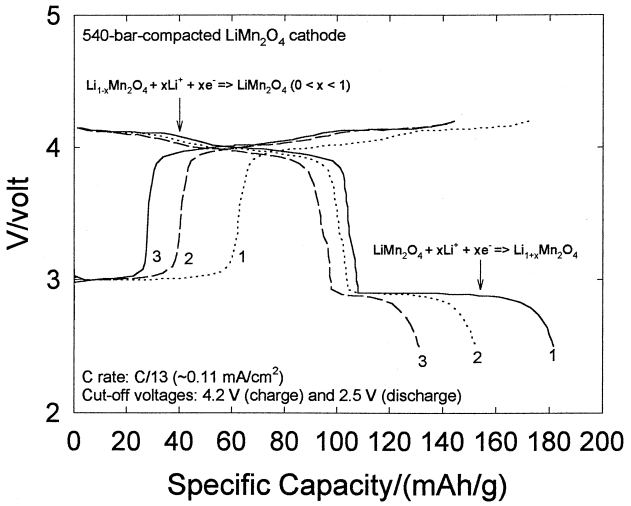

Fig. 9. Charge and discharge behavior of rechargeable lithium cells using a $LiMn_2O_4$ cathode prepared with 540-bar compaction. The cut-off voltages were 4.2 V for charge and 2.5 V for discharge. The capacity-rate was $C/13$ (~ 0.11 mA/cm^2).

540 bar and cycled at a $C/13$ rate (~ 0.11 mA/cm^2). It was found (not shown) that a cell using a cast cathode could not be cycled, even at a rate as slow as $C/100$ (~ 0.015 mA/cm^2). The lithium intercalation and deintercalation reaction at ~ 2.9 V ($LiMn_2O_4 + xLi^+ + xe^- \Leftrightarrow Li_{1+x}Mn_2O_4$ $(0 < x < 1)$) is not reversible, which confirms a previous finding [16]. This irreversibility lowers the reversible capacity (~ 4 V) most likely because of an adverse effect on the spinel structure of $LiMn_2O_4$.

Fig. 10 shows the charge and discharge behavior of a rechargeable lithium cell using a $LiMn_2O_4$ cathode at $C/13$ rate (~ 0.11 mA/cm^2) with the cut-off voltage of 3 V (discharge) and 4.2 V (charge). Note that, in contrast to Fig. 9, there is no capacity decline. Clearly, a cell based on a $LiMn_2O_4$ cathode can not be cycled below 3 V. The lithium cell using 540-bar-compacted cathode showed the

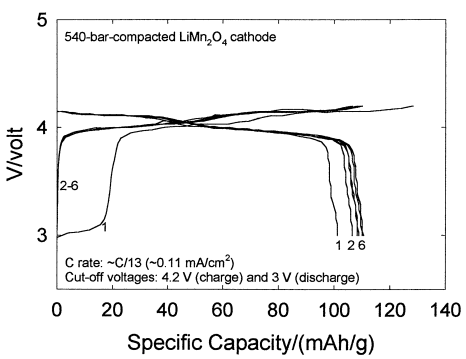

Fig. 10. Charge and discharge behavior of rechargeable lithium cells using a $LiMn_2O_4$ cathode prepared from 540-bar compaction. The cut-off voltages were 4.2 V for charge and 3 V for discharge. The C rate was $C/13$ (~ 0.11 mA/cm^2).

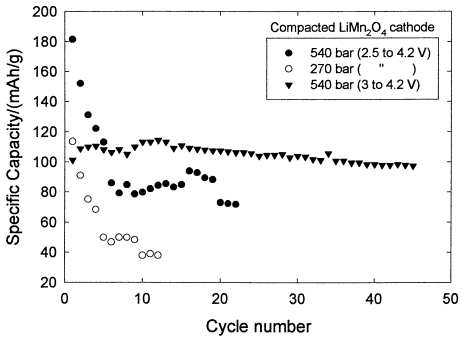

Fig. 11. Capacity dependence on cycle number for lithium cells using a $LiMn_2O_4$ cathode. For the 540-bar-compacted-cathode cell cycled between 3 and 4.2 V, the C rates were $\sim C/13$ (~ 0.11 mA/cm^2) for cycles 1 to 10, $\sim C/26$ (~ 0.057 mA/cm^2) for cycles 12 to 15, $\sim C/9$ (~ 0.17 mA/cm^2) for cycles 15 to 46. For the 540-bar-compacted-cathode cell cycled between 2.5 and 4.2 V, the C rates were $\sim C/13$ (~ 0.11 mA/cm^2) for cycles 1 to 14, $\sim C/26$ (~ 0.056 mA/cm^2) for cycles 15 to 19, $\sim C/9$ (~ 0.17 mA/cm^2) for other cycles. For the 270-bar-compacted-cathode cell cycled between 2.5 and 4.2 V, the C rate was $\sim C/26$ (~ 0.056 mA/cm^2) for cycles 6 to 9, $\sim C/9$ (~ 0.17 mA/cm^2) for other cycles.

highest capacity, which can be seen more clearly in Fig. 11.

4. Discussion

4.1. Electrochemical impedance spectra

4.1.1. Uncycled cells

An interesting EIS result (Figs. 1, 5 and 8) is that the radius of Arc A for uncycled cells decreases with increase in compaction pressure. This observation suggests that Arc A, to a degree, may be ascribed to the cathode compaction, which has not been previously reported to our knowledge. In past studies [2,17,18], the high-frequency semicircle (Arc A) was considered mainly to originate from the interfacial impedance of the lithium anode. Since Arc A was in the relatively high-frequency range, the cathode contribution to Arc A might be from compaction of the cathode in a thin layer adjacent to the electrolyte. Under the high-compaction pressure, the surface coverage of PVDF on the metal oxide and carbon particles can decrease and, consequently, effect a decrease in resistance (i.e., radius of Arc A). Arc A may also contain a contribution from a passive film on the oxide particle surface (caused by the reaction between oxide and electrolyte). Therefore, in our following proposed circuit model, contributions from the surface layer of the composite cathode are also considered.

Arc B also decreases with increase in compaction pressure (Figs. 1, 5 and 8). In view of Arc B being in the low-frequency range, this decrease suggests that Arc B mainly contains a contribution from compaction within the composite cathode, i.e., the inter-particle contacts such as oxide–oxide, carbon–oxide, and carbon–carbon grain contacts. This suggestion differs from the view of Popov et al. [18] of the low-frequency semicircle who considered that Arc B for a Li/BCX cell was a Warburg impedance caused by the Li/electrolyte interface, as evidenced by the ascending slope of $\sim 45°$ of Arc B at the real axis. Any contribution from the cathode was ruled out because the slope for a Warburg impedance for a porous electrode would be 22.5° [19].

We attribute Arc B mainly to cathode effects because its radius decreases with compaction pressure. The slope of the ascending portion of Arc B is in the range 39–55° (except for Fig. 8b) for all cathodes which indicates a common physical origin, e.g., inter-particle contact [1]. The lower angle of $\sim 17°$ in Fig. 8b is probably due to overlap between Arc A and Arc B.

As mentioned above, the PVDF binder should be an important factor in explaining the effect of compaction pressure on Arc A and Arc B for the uncycled cells. It is reasonable to assume that the PVDF coverage of the oxide and carbon particles diminishes as the composite cathode is compacted at an increasing pressure. A large PVDF coverage on the oxide and carbon particles would lead to poor inter-particle contact and, consequently, a low electronic conductivity, which will have an adverse effect on the capacity and capacity-dependence on C rate. We discuss this point in Section 4.2.

4.1.2. Cycled cells

It appears that the compaction pressure has no effect on EIS results for cycled cells. This observation suggests that PVDF is no longer a factor in causing a large resistance. This is a reasonable inference because PVDF can swell in an electrolyte solution [20]. Because PVDF is plasticized by the electrolyte, its ionic resistance should decrease substantially. In addition, the cathode passive film can be destroyed during the discharge process [3,18], which will also effect a smaller resistance. In view of this discussion, it is not surprising to see a decrease in the radii of Arcs A and B for cycled cells. It should be pointed out that electronic conductivity in the composite cathode should not be effected by PVDF swelling with electrolyte. It is also reasonable to expect that the inter-particle contact does not change substantially upon cycling. Actually, it is our opinion that the compaction pressure strongly effects the inter-particle contact, as discussed in Section 4.2.

It seems that Arc A in a cycled cell mainly contains contributions from the passive film on the lithium anode, and Arc B mainly contains contributions from grain boundaries in the composite cathode. However, there are still some differences among the Arcs A obtained from the cycled cells, which are discussed further below.

For the cycled cells using a $LiCoO_2$ cathode (Fig. 5b), it appears that Arc A is a well-defined semicircle. Such behavior is not surprising because the EIS is also a well-defined semicircle for a cell Li/electrolyte/Li after pas-

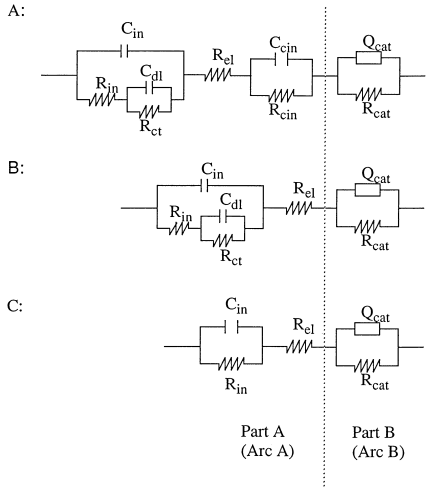

Fig. 12. The proposed equivalent circuit models. Model A is for uncycled cells. Model B is for cycled cells using $LiNiO_2$ and $LiMn_2O_4$ cathodes. Model C is for $LiCoO_2$-based-cycled cell at 270 bar.

sage of 0.1 Ah, followed by 24-h open-circuit equilibration [2]. This observation is indirect support for our argument that Arc A is mainly caused by the interfacial impedance between lithium and electrolyte.

For the cycled cells using $LiMn_2O_4$ and $LiNiO_2$ cathodes, Arcs A are not well-defined semicircles which suggests that there remains a contribution from the passive cathode film. If there is a contribution to Arc A from the cathode, this suggests that $LiNiO_2$ and $LiMn_2O_4$ are so reactive that the cathode passive film is reformed within a short time after discharge.

4.1.3. Equivalent circuit model

Considering the above discussion on the origin of Arcs A and B, as well as the studies of Koksbang et al. [1], Narayanan et al. [2], Thomas et al. [17], and Popov et al. [18], the proposed equivalent circuit models (ECM) are shown in Fig. 12a (uncycled cells), Fig. 12b and Fig. 12c (cycled cells). These ECMs are divided into Part A (fitting Arc A) and Part B (fitting Arc B). In Part A, R_{el} is the resistance of electrolyte; R_{in} and C_{in} are the resistance and capacitance of the passive film of the lithium surface, respectively; R_{ct} and C_{dl} are the charge-transfer resistance and double-layer capacitance of the lithium/electrolyte interface, respectively; R_{cin} and C_{cin} are the resistance and capacitance of the passive film on the cathode surface, respectively. In Part B, R_{cat}, Q_{cat}, and n are, respectively, the resistance, the constant phase element (CPE) impedance, and corresponding power factor related to the porous composite cathode. A CPE is commonly used to describe the complicated EIS results from a porous electrode, which is evidenced by Arc B generally not being a well-defined semicircle (Figs. 1, 5 and 8). The contribution from charge-transfer resistance for the lithium intercalation process can be neglected because it is small compared with other contributions [1].

Table 2
Results from fitting the obtained EIS data to the equivalent circuits shown in Fig. 12

Bar	Cycle	R_{el} (Ω)	$C_{in} \times 10^6$ (F)	R_{in} (Ω)	R_{ct} (Ω)	$C_{dl} \times 10^6$ (F)	R_{cin} (Ω)	$C_{cin} \times 10^6$ (F)	R_{cat} (Ω)	$Y_{cat}^b \times 10^3$ (mho)	n
(a) $LiNiO_2$											
0 (cast)	0[c]	10									
270	0	17.9	0.4	12.4	32.3	7.26	69.1	0.44	10^{19}[d]	2.56	0.59
	7	11	1.9	7	3	33.4			33	5.0	0.8
540	0	19.4	1.57	7.77	11.5	95	28.1	6.4	4189	2.82	0.67
	7	8.1	1.6	7.8	3.3	78.5			80.9	8.7	0.67
(b) $LiCoO_2$											
0 (cast)	0[c]	9									
270	0	25	1.1	42	35	11	11	0.9	[a]	[a]	[a]
	15	7	1.1	17					21	3.28	0.9
540	0	40	9.5	14	7	100	15	0.4	[a]	[a]	[a]
	15	7	1.3	7	2	101			37	4.75	0.9
(c) $LiMn_2O_4$											
0 (cast)	0[c]	12									
270	0	22	0.91	47.3	15.8	11	16.3	0.27	236	1.49	0.43
	8	19	0.27	21	33	152	25	4	[e]	[e]	[e]
540	0	10.2	5.51	24	20	37.9	5	3.5	200	8.9	0.46
	8	10.1	0.3	35.5	11.8	25.3			67.7	57.5	0.62

[a] The data were collected in the frequency range 100 kHz to 10 Hz in which Arc B did not develop well enough to fit R_{cat} and Q_{cat}.
[b] $Q_{cat} = Y_{cat}^{-1}(j\omega)^{-n}$.
[c] These EISs were not fitted because Arcs A and B did not separate well. It was found that the spectra changed little either after the cells were stored at room temperature for weeks or after the cells were heated at 60°C for several hours. This observation suggests that most of the cathode particles are covered completely by a PVDF film since the plasticized PVDF did not cause a significant decrease in the impedance.
[d] This large resistance is not physically meaningful but results from forcing a fit for Arc B.
[e] Arc B did not develop well enough to fit R_{cat} and Q_{cat} in the frequency range 100 kHz to 0.1 Hz.

The fitting results are summarized in Table 2. The parameters obtained from the fitting concur with the above discussion. For instance, R_{cin} and R_{cat} of the uncycled cells using 270-bar compacted cathodes are larger than those of uncycled cells using 540-bar compacted cathodes. In contrast, R_{cin} and R_{cat} for the cycled cell have no such tendency.

4.2. Cell capacity and its relation to EIS results

The capacities of the cathodes studied are quite good. For example, the capacity for $LiMn_2O_4$ is around ~ 96 mAh/g ($\sim 65\%$ of its theoretical value 148 mAh/g [12]) at $\sim C/9$ after ~ 50 cycles. This capacity is near the practical limit (~ 110 mAh/g) [21]. The capacity of $LiCoO_2$ is ~ 106 mAh/g ($\sim 77\%$ of its theoretical value 137 mAh/g [12]) at $\sim C/12$ rate after ~ 50 cycles. The capacity of $LiNiO_2$ is ~ 135 mAh/g (70% of its theoretical value 192 mAh/g [12]) at $\sim C/10$ after ~ 40 cycles.

There is, however, a need to improve the capacity at higher C rates for $LiNiO_2$. As seen in Fig. 4, it has the greatest decrease in capacity with C rate. This observation does not seem congruent with lithium diffusion coefficients available in the literature. The capacity dependence on C rate should be the least (or comparable) for cells using $LiNiO_2$ compared with $LiCoO_2$ and $LiMn_2O_4$ cathodes because the lithium diffusion coefficient in $LiNiO_2$ is $\sim 2\times 10^{-7}$ cm^2 s^{-1} [22] (or $\sim 10^{-8}$ cm^2 s^{-1} [23]) the highest (or comparable) value among the studied cathode materials [15]. This unexpected result may be caused by the $LiNiO_2$ particles being the largest, as suggested by the fact that the cast or compacted $LiNiO_2$ cathode was the roughest among the three (Table 1). A large particle size usually results in a poor C rate because the specific surface area of the particle is small [21].

The correlation between the capacity and EIS results is clear: cells using cathodes compacted at 540 bar show the highest capacity and the smallest resistance for the uncycled cell (i.e., smallest radii of Arc A and Arc B), and cells using a cast cathode show essentially a zero capacity and an exceptionally large resistance. These results may be attributed to the effect of compaction pressure on the PVDF binder: PVDF can result in poor inter-particle contact (i.e., oxide–oxide, carbon–oxide, carbon–carbon) if the composite cathode is cast only or compacted at a low pressure. The poor oxide–oxide inter-particle contact will lead to poor lithium transport between the oxide particles; but poor inter-particle transport is unlikely to be the origin for observing the correlation between capacity and EIS results because the liquid electrolyte provides the predominant pathway for lithium diffusion into the active oxides. The carbon–oxide and carbon–carbon inter-particle contact is thought to be the physical origin for the observed pressure–performance correlation. Poor carbon–oxide and carbon–carbon inter-particle contact will lead to a poor electronic conductivity in the composite cathode, which is confirmed by the observation that the measured apparent electronic conductivity of the cast $LiMn_2O_4$ cathode ($\sim 10^{-7}$ Scm^{-1}) is much smaller than that obtained with the 540-bar-compacted $LiMn_2O_4$ cathode ($\sim 10^{-4}$ Scm^{-1}). (The electronic conductivity of the composite cathode was estimated from the resistance measured for a composite cathode disk placed between two metal plates.) In addition, oxide particles covered completely by PVDF will not be available in the charge and recharge process (no electronic conductive path). From this point of view, to obtain good performance from the composite cathode in lithium batteries, a cast cathode must be compacted even though compaction will decrease the porosity. The compaction is good if Arc B is smallest, and the expected capacity will be high.

4.3. C rate and its relation to EIS results

Combining the information in Figs. 1 and 4, as well as Table 2, a correlation is seen between R_{cat} and the capacity dependence on C rate. The capacity decrease (Fig. 4) with increasing C rate for the uncycled cell using a $LiNiO_2$ cathode is greater than for the corresponding cycled cell. Commensurately, R_{cat} for the uncycled cell with a $LiNiO_2$ cathode is 288 times larger than that for the cycled cell (4189 vs. 18 Ω). That is, the higher C-rate performance corresponds to the smaller R_{cat}. This is probably because liquid electrolyte does not penetrate into the PVDF film covering the $LiNiO_2$ particle in the uncycled cells (in the time frame of the experiment), and, hence, limiting the active oxide accessible for charge and discharge. The dramatic decrease in the resistance R_{cat} suggests that electrolyte has wetted the PVDF film in the cycled cells. The wetted composite cathode will have higher apparent lithium diffusion coefficient which can effect a higher C rate [15].

For the $LiCoO_2$- and $LiMn_2O_4$-based cells, the liquid electrolyte may penetrate into these two composite cathodes relatively fast perhaps because the PVDF film covering the particles is thinner. This is supported by the observation that R_{cat} (Table 2) of the uncycled cells for $LiMn_2O_4$-based cells are only several times larger than those of the cycled cells. (Data were not collected for $LiCoO_2$ at sufficiently low frequency to fit R_{cat}.) Therefore, in the tested C-rate range, the capacity dependence on C rate is similar for the uncycled cell and cycled cells. Perhaps, a difference can be seen at a higher C-rate than studied here.

5. Conclusions

The high-frequency arc of EIS results obtained from lithium cells studied is due to a combination of the Li/electrolyte and cathode/electrolyte interface, and that the low-frequency arc is due to grain boundaries in the

composite cathode. To ensure high capacity at a high *C* rate, the resistance of the uncycled cell at low frequencies must be as small as possible. This implies that the performance of lithium cells can be gauged by EIS without cycling the cell, which may save time in the development of high-capacity lithium batteries. The cast cathode must be compacted prior to its use, even though the compaction will decrease the cathode porosity. Of course, the compaction pressure cannot be increased without limit because too little porosity in the composite cathode will cause a performance decline. The liquid electrolyte absorbed by the binder PVDF is critical for the performance of the composite cathode.

Acknowledgements

We thank DOE for financial support (DE-FG05-94ER14495), Dr. Robert Spotnitz (Hoechst Celanese) for allowing us to cast cathodes in his laboratory and supplying Al and Cu foil current collector, and Mr. Brad Johnson (University of South Carolina) for his assistance in casting the cathodes. We also thank Ms. Xi-Yun Yu for measuring and fitting the EIS results.

References

[1] R. Koksbang, I.I. Olsen, P.E. Tonder, N. Knudsen, D. Fauteux, J. Appl. Electrochem. 21 (1991) 301.
[2] S.R. Narayanan, D.H. Shen, S. Surampudi, A.I. Attia, G. Halpert, J. Electrochem. Soc. 140 (1993) 1854.
[3] G. Pistoia, A. Antonin, R. Rosati, D. Zane, Electrochimica 141 (1996) 2683.
[4] C.D. Desjardins, K. Maclean, J. Electrochem. Soc. 136 (1986) 345.
[5] G. Montesperelli, P. Nunziante, M. Pasquali, G. Pistoia, Solid State Ionics 37 (1990) 149.
[6] J. Fan, P.S. Fedkiw, J. Electrochem. Soc. 144 (1997) 399.
[7] M. Gaberscek, S. Pejovnik, Electrochim. Acta 41 (1996) 1137.
[8] F. Capuano, F. Croce, B. Scrosati, J. Electrochem. Soc. 138 (1991) .
[9] J.S. Xue, J.R. Dahn, J. Electrochem. Soc. 142 (1995) 3668.
[10] A.R. Armstrong, P.G. Bruce, Nature 381 (1996) 499.
[11] D.B. Le, S. Passerini, A.L. Tipton, B.B. Owens, W.H. Smyri, J. Electrochem. Soc. 142 (1995) L102.
[12] K. Brandt, Solid State Ionics 69 (1994) 171.
[13] R. Kanno, H. Kudo, Y. Kawamoto, T. Kamiyama, F. Izumi, Y. Takeda, M. Takano, J. Solid State Chem. 110 (1994) 216.
[14] S.-Y. Huang, Adv. Battery Technol. 132 (1996) 8.
[15] B. Scrosati, in: J. Lipkowski, P.N. Ross (Eds.), Electrochemistry of Novel Materials Frontiers of Electrochemistry, Chap. 3, VCH Publishers, New York, p. 111.
[16] Z. Jiang, K.M. Abraham, J. Electrochem. Soc. 143 (1996) 1591.
[17] M.G.S.R. Thomas, P.G. Bruce, J.B. Goodenough, J. Electrochem. Soc. 132 (1989) 345.
[18] N. Popov, W. Zhang, E.C. Darcy, R.E. White, J. Electrochem. Soc. 140 (1993) 3097.
[19] N. Matsui, J. Power Sources 20 (1987) 135.
[20] J.S. Humphrey, N. Margalit, in: The Proceedings of the 12th International Symposium on Primary and Secondary Battery Technology and Applications, Deerfield Beach, FL, USA, March 6–9, 1995.
[21] L. Xie, D. Fouchard, S. Megahed, Mat. Res. Soc. Symp. Proc. 393 (1995) 285.
[22] P.G. Bruce, A. Lisowska-Oleksiak, M.Y. Saidi, C.A. Vincent, Solid State Ionics 57 (1985) 353.
[23] B. Jerry, K.-B. Rene, S.M. Yazid, Solid State Ionics 89 (1996) 25.